Solar PV Array fed Speed Sensor less Vector Control of Induction Motor Drive for Water Pumping

MOHD MUDASSIR HUSSAIN [1], K.RAJEEV [2], P.NAGESWARA RAO [3]

[1] *PG student, Department of Electrical And Electronic ,Vidya Jyothi Institute of Technology ,Hyderabad, India*
[2] *ASSISTANT PROFESSOR, Department of Electrical And Electronic ,Vidya Jyothi Institute of Technology ,Hyderabad, India*
[3]*ASSOCIATE PROFESSOR, Department of Electrical And Electronic ,Vidya Jyothi Institute of Technology ,Hyderabad, India*

ABSTRACT

This paper shows a sun based PV cluster bolstered speed sensor-less vector controlled enlistment engine drive for water pumping framework. To harness greatest conceivable power from sun oriented PV exhibit, a DC-DC converter is utilized. The delicate beginning of the engine is accomplished to moderate exchanging worry of the converter and afterward the most extreme power is followed utilizing a notable annoy and watch (P and O) control calculation. With every single due righteousness related with the acceptance engine regarding the heap attributes, it is induced that this engine is most appropriate to drive a water pump having non-straight torque-speed trademark and it is watched that the execution is far better than the DC engine. The coveted arrangement is planned and reproduced in MATLAB/Simulink stage and the outline and control of the framework are approved through showing of reenactment comes about.

Keyword : - *Speed sensor-less control, Stator field-oriented vector control, Solar photovoltaic (PV), P&O MPPT control, Induction motor, Water pump.*

1. INTRODUCTION

The ever increasing demand of electrical energy and limited availability of non-renewable sources of energy have motivated the researchers to search for the new options [1]. Hence, it has been mandatory to utilize the solar energy for various purposes [2]. The evolution of power electronics devices has further reduced the difficulties to properly utilizing this energy for different applications. One of the most widely used application of solar PV array is water pumping [3-4].

In its crude stage sun based PV water pumping has been acknowledged utilizing the DC engine. Be that as it may, because of inborn confinement of a DC engine based water pumping framework it has been supplanted by an acceptance engine as it is mechanically straightforward, rough, and dependable and it has minimal effort, high proficiency, low upkeep than the DC engines. Here a two phase control of sun oriented PV exhibit bolstered acceptance engine drive utilizing vector control is utilized [5-6]. To start with organize incorporates the control of a lift converter for MPPT of PV exhibit. DC-DC converters assume an essential part in the PV framework. As one most likely is aware power created by PV framework relies upon sun based insolation and temperature. Normal for PV module displays a solitary power crest. In this way, the calculation for following most extreme conceivable power is utilized and the PV exhibit is worked at that power.

The boost converter is used as a circuit to match the impedance between the PV panel and the load such that the total power transmitted from the PV array must reach the load. Hence, the suitability and selectivity of boost converter are must. A vast comparative analysis has been performed in terms of complexity, computation time and efficiency of DC-DC converters [7-8]. A number of DC-DC converters which have been frequently used for solar PV based water pumping purpose are buck, boost, buck-boost converters etc. Here, perturb and observe MPPT algorithm has been used to track MPPT. It is most commonly used MPPT algorithm especially for low cost

implementation. The only drawback of this algorithm is the operating point oscillation around MPP in steady-state giving rise to waste of some amount of available energy [9]. The second stage includes DC-AC conversion with voltage source inverter (VSI) feeding vector-controlled three-phase induction motor drive.

The languid reaction of the enlistment engine in light of utilizing scalar control can be tackled by utilizing vector control [10-12]. The field-arranged control implies that an AC engine will undoubtedly carry on powerfully as a DC engine by utilizing input control [13]. This strategy additionally gives the chance to fluctuate the speed over the wide range. Subsequently with the utilization of effective microcomputer and DSPs, the vector control expels scalar control [14-15]. In addition, sensor-less control of the drive guarantees the materialness of the engine where great execution with minimal effort is required. In the stator field-situated vector control plot, the motion is evaluated which is utilized to gauge the slip speed (Ȧsl) and synchronous speed (Ȧe) which is additionally used to appraise the engine speed. The execution of the proposed framework is accomplished through reenactment utilizing MATLAB/Simulink. Reenactment comes about check suitability of proposed framework for this reason.

2. SYSTEM CONFIGURATION

Fig.1 represents the solar PV fed speed sensor-less vector controlled induction motor drive for water pumps. This configuration involves solar PV array followed by the boost converter to achieve MPPT of PV array. It is then supplied to a three phase induction motor drive driving an irrigation pump via three phase voltage source inverter. The motor speed I estimated through the rotor flux which is estimated by DC link voltage and it is utilized for generation of switching pulses for controlling the inverter switches by vector control. Perturb and observe (P&O) control algorithm is used for MPPT to generate switching pulse to boost converter switch as shown in Fig.3.
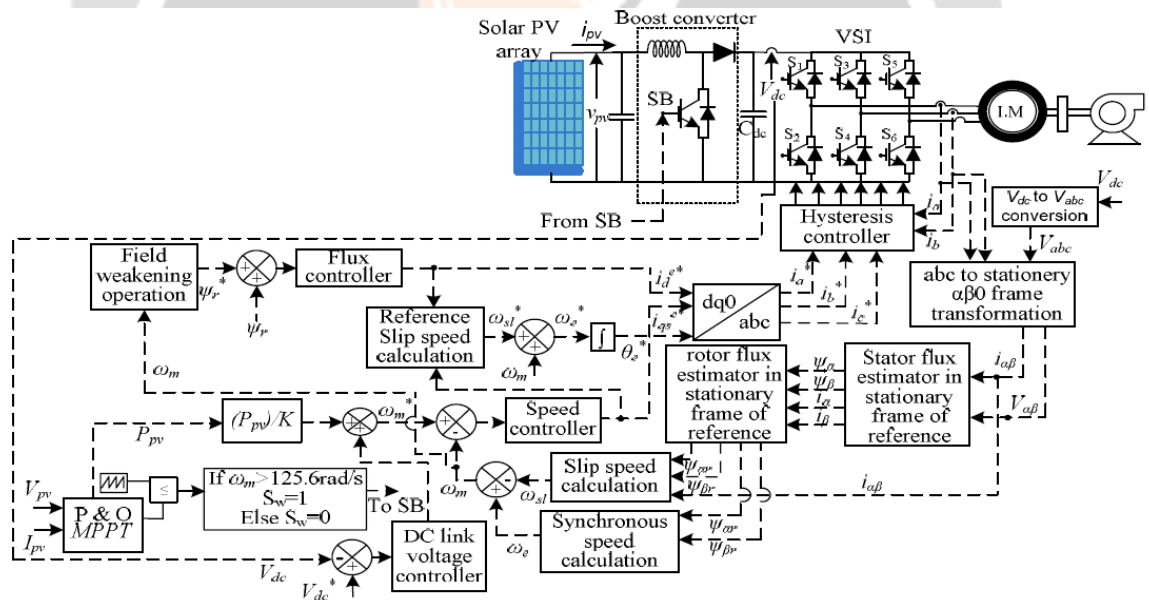

Fig. 1. Schematic Diagram of solar PV fed vector controlled induction motor Drive

3. DESIGN OF SYSTEM

Fig.1 shows a three-phase induction motor of 3.7 kW (5 HP), 415V which is used to drive the pump. This purpose can be fulfilled by using a 4.5 kW maximum solar PV array power. The design of various stages of proposed system is given here and the performance of overall system is shown in subsequent sections under various conditions. The detailed data are given in Appendices.

A. Design of Solar PV Array

A 4500 W solar PV array is designed to feed the pump. For this purpose, a solar module consisting of 36 cells of open circuit voltage (Voca) of 21.6Vand 0.64A short circuit current (Isca) is designed to give above rating by connecting Nser numbers of series connected modules and Npar numbers of parallel connected module.

$$P_{mpp} = (N_{ser} \times V_{mpp}) \times (N_{par} \times I_{mpp}) = 4.5\,kW \qquad (1)$$

Where Vmpp=solar PV voltage at maximum power and Impp=solar PV current at maximum power. Here 10W, 17.6V (Vmpp), 0.58A (Impp) module is selected for this purpose as shown in Fig.2.

It has been examined that Vmpp=0.85*Voca and Impp=0.90*Isca. Hence Pmpp for one module is given by Pmpp=Vmpp*Impp.

Now Voc=600V, the number of series connected module (Nser)= Voc/Voca= 600/21.6§29 and number of parallel connected modules are (Npar) = P mpp/(0.85*Voc*Impp)= 4500/ [(0.85*600)*0.58]=15.25§16.

By this way connecting 29 modules in series and 16 modules in parallel one can achieve 4500W solar PV array (29*60) with 600V and 8.7A.
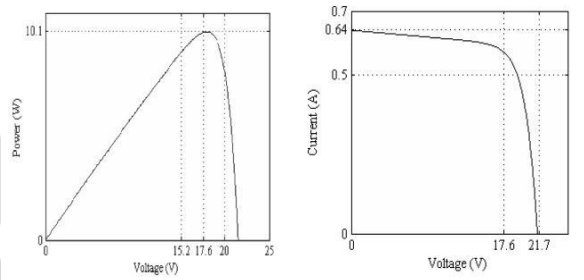

Fig. 2. Power vs Voltage and Current vs Voltage curve for one module

B. Calculation of DC Link Voltage

In order to control the output current of VSI, the voltage of the DC link should be more as compared to the peak amplitude of line-line voltage rating of the motor.

$$V_{dc} = \sqrt{2} \times V_L = \sqrt{2} \times 415 = 587V \qquad (2)$$

The selected value as DC link voltage is 600V.

C. Design of Boost Inductor

The obligation proportion (D) for the lift converter is observed to be 0.1 by the accompanying connection.

$$V_o = \frac{V_{in}}{(1-D)} \quad \text{or} \quad D = \frac{V_0 - V_{in}}{V_0} = 1 - \frac{540}{600} = 0.1 \qquad (3)$$

Hence, the boost converter inductor can be calculated as follows,

$$L_1 = \frac{V_{mpp} \times D}{\Delta I_1 \times f_s} = \frac{540 \times 0.10}{.25 \times 8.7 \times 10000} \approx 2.5mH \qquad (4)$$

Where fs is the switching frequency and åI1 is the ripple allowed in the current.

D. Design of DC Link Capacitor

The value of DC link capacitor is estimated by using fundamental frequency as [12],

$$\omega_{rated} = 2 \times \pi \times f_{rated} = 2 \times \pi \times 50 = 314\,rad\,/\,s \qquad (5)$$

$$\frac{1}{2} \times C_{dc} \times (V_{dc}^2 - V_{dc1}^2) = 3aV_p It = 3 \times 1.2 \times 239.6 \times 8.7 \times .005 \qquad (6)$$

Hence, Cdc = 2890.7µ F

Where Vdc is the DC interface voltage and Vdc1 is the base voltage, t is the time required for the voltage to get diminished to least permissible DC-connect voltage, I is the stage current of the engine and Vp is the stage voltage. The capacitor esteem is chosen as 3000 $_3$F.E. Design of Water Pump

To pump water radiating pump is being utilized here in which the created stack torque (TL) is straightforwardly in extent to the square of the engine speed. Henceforth the proportionality steady is figured as takes after

$$K_1 = \frac{T_L}{\omega_p^2} = \frac{12.5}{299.8^2} = .000137 \, Nm/(rad/s)^2 \qquad (7)$$

4. CONTROL OF THE SYSTEM

The control of general framework incorporates MPPT of sun based PV cluster to separate most extreme power through a lift converter, help converter exchanging by utilizing hysteresis-controller for vector control of IMD (Induction Motor Drive) and speed estimation for speed sensor-less vector control of an enlistment engine drive.

A. Perturb and Observe (P&O) Algorithm

The system for controlling the sun oriented PV cluster voltage is given in Fig.3. The obligation cycle is created by contrasting it and the saw-tooth rehashing grouping and it is balanced in such an approach to track most extreme power purpose of the sun based PV exhibit control versus voltage bend. In this MPPT plot, the PV voltage and PV current are acquired at every cycle and the relating power is ascertained. On the off chance that the result of sun based PV power and voltage is more than the last cycle item then the estimation of sun based PV voltage is expanded and new esteem is refreshed generally PV voltage esteem is diminished and new estimation of voltage is refreshed.

It has been watched that there is a backwards connection between the obligation proportion (D) of the lift converter and the PV voltage. In this way, when the PV voltage expands, the obligation proportion (D) declines and the other way around. The obligation proportion along these lines acquired is contrasted with the saw-tooth waveform with produce exchanging heartbeats for support converter switch (SB).

The PV power can be converted into speed by the following relation and this gives one component of the speed by affinity law of pump and it is expressed by the following formula.

$$\omega_1 = \frac{P_{pv}}{K_1} \, rad/s \qquad (8)$$

Where K1 is proportionality constant of pump. The second component of reference speed is estimated by DC-link voltage PI controller of VSI. The DC-link voltage error is obtained as,

$$V_{dcl(k)} = V^*_{dc(k)} - V_{dc(k)} \qquad (9)$$

The error signal Vdcl(k) is fed to the DC link voltage PI controller the output of which is speed signal at the kth sampling instant and is given as follows,

$$\omega_{2(k)} = \omega_{2(k-1)} + K_{pdc}\{V_{dcl(k)} - V_{dcl(k-1)}\} + K_{idc}V_{dcl(k)} \qquad (10)$$

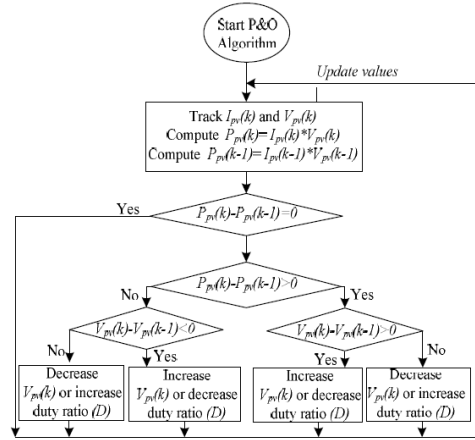$$\omega^*_m = \omega_1 + \omega_2 \qquad (11)$$

Fig. 3. Perturb and Observe control algorithm

B. Speed Estimation of Induction Motor Drive The fundamental equation for the estimation of speed is given as following. The DC link voltage (Vdc) is used to find out three phase voltages by the given expression.

$$v_a = \frac{V_{dc}}{3}\left(2S_a - S_b - S_c\right), v_b = \frac{V_{dc}}{3}\left(2S_b - S_a - S_c\right)$$

$$v_c = \frac{V_{dc}}{3}\left(2S_c - S_b - S_a\right) \tag{12}$$

Where Sa, Sb and Sc are switching functions (which are either one or zero) of VSI. The various voltage and current transformation equations to transform from abc to αβδ domain are given as,

$$v_\beta = \frac{2}{3}\left(v_a - \frac{v_b}{2} - \frac{v_c}{2}\right), v_\alpha = \frac{1}{\sqrt{3}}\left(-v_b + v_c\right) \tag{13}$$

$$i_\beta = \frac{2}{3}\left(i_a - \frac{i_b}{2} - \frac{i_c}{2}\right), i_\alpha = \frac{-1}{\sqrt{3}}\left(2i_b + i_a\right) \tag{14}$$

$$\psi_\beta = \int\left(V_\beta - R_s * i_\beta\right)dt, \psi_\alpha = \int\left(V_\alpha - R_s * i_\alpha\right)dt \tag{15}$$

$$\psi_s = \sqrt{\psi_\alpha^2 + \psi_\beta^2} \tag{16}$$

The rotor flux component in stationery reference frame is given as,

$$\psi_{\alpha r} = \left(\psi_\alpha - i_\alpha * L_{ls}\right)\frac{L_r}{L_m} - i_\alpha L_{lr} \tag{17}$$

$$\psi_{\beta r} = \left(\psi_\beta - i_\beta * L_{ls}\right)\frac{L_r}{L_m} - i_\beta L_{lr} \tag{18}$$

$$\psi_r = \sqrt{\psi_{\beta r}^2 + \psi_{\alpha r}^2} \tag{19}$$

Where Lr=rotor inductance, Lm=magnetizing inductance, Llr=rotor leakage inductance, Lls=stator leakage inductance, Rr=stator referred rotor resistance, Rs=stator resistance.

$$\omega_{sl} = \frac{L_m}{T_r}\left\{\frac{i_\beta\psi_{\alpha r} - i_\alpha\psi_{\beta r}}{\psi_r^2}\right\} \tag{20}$$

$$\omega_e = \frac{\psi_{\alpha r}\, p\psi_{\beta r} - \psi_{\beta r}\, p\psi_{\alpha r}}{\psi^2} \tag{21}$$

The motor speed is given as

$$\omega_m = \omega_e - \omega_{sl} \qquad (22)$$

C. Field Weakening Control

If the induction motor speed is less than the base speed of the motor , then the direct-axis current is as,

$$I_{ds}^{e\,*} = I_{mag} \qquad (23)$$

If the induction motor speed is greater than the base speed of the motor, the operation of flux-weakening is performed. The estimated rotor speed is related to the magnetizing current in the flux-weakening region by the equation given as,

$$I_{ds}^{e\,*} = \frac{\omega_{base}}{\omega_m} I_{mag} \qquad (24)$$

Where Imag is the rated magnetizing current of the motor.

D. Vector Control of Induction Motor Drive

As mentioned above, the vector control method is used to control the stator currents and flux. It comprises of three stages, Flux component of current vector (Ids *) is calculated as,

$$I_{ds}^{*} = I_{ds}^{e*} + T_r \times p I_{ds}^{e*} \qquad (25)$$

Where Tr =Lr/Rr = rotor time-constant.

$$\omega_{error} = \omega_m^* - \omega_m \qquad (26)$$

$$T_{e(k)}^{*} = T_{e(k-1)}^{*} + K_{p\omega}\left\{\omega_{error(k)} - \omega_{error(k-1)}\right\} + K_{i\omega}\omega_{error(k)} \qquad (27)$$

$$I_{qs}^{e*} = \frac{T_e^{*}}{K \times I_{ds}^{e*}} \qquad (28)$$

Where, K=(3PLm)/4Lr, Lr is rotor inductance, Lm is the magnetizing inductance, P is the number of poles.

$$\omega_{sl}^{*} = \frac{I_{qs}^{e*}}{T_r * I_{ds}^{e*}} \qquad (29)$$

This reference slip speed (ωsl) is added with the estimated speed (ωm) to calculate reference synchronous speed (ωe) in rad/s.

$$\omega_e^{*} = \omega_m + \omega_{sl}^{*} \qquad (30)$$

The synchronous speed thus calculated is used to get flux angle (ωe) at the kth

$$\theta_{e(k)} = \theta_{e(k-1)} + \omega_e^{*} \times T \qquad (31)$$

Where T=Sampling period of the signal.

The value of q-axis and d-axis current components Ids e* and Iqs e* respectively obtained from (25) and (28), are used to obtain reference phase currents ia *, ib *, ic * by following equations,

$$i_a^{*} = I_{ds}^{e*}\sin\theta_e + I_{qs}^{e*}\cos\theta_e \qquad (32)$$

$$i_b^{*} = I_{ds}^{e*}\sin\left(\theta_e - \frac{2\pi}{3}\right) + I_{qs}^{e*}\cos\left(\theta_e - \frac{2\pi}{3}\right) \qquad (33)$$

$$i_c^{*} = I_{ds}^{e*}\sin\left(\theta_e + \frac{2\pi}{3}\right) + I_{qs}^{e*}\cos\left(\theta_e + \frac{2\pi}{3}\right) \qquad (34)$$

reference phase currents (ia *, ib *, ic *) are compared with the sensed phase currents (ia, ib, ic) and the error signal is passed through hysteresis-band controller to generate switching pulses for inverter switches.

5. RESULT AND DISCUSSION

The proposed solar PV fed vector controlled induction motor drive is modeled for water pumping system and its simulation has been performed in MATLAB/ Simulink using SPS toolbox. The salient points of these results are as follows.

A. Starting and Steady-State Performance

Fig.4 to Fig.6 speak to the beginning exhibitions of sun oriented PV sustained vector controlled acceptance engine drive at a settled protection of 1000W/m2. Fig.4 speaks to the sun oriented PV cluster parameters, for example, sun based PV voltage (Vpv), PV current (Ipv), PV control (Ppv), DC interface voltage (Vdc) and inductor current. It is watched that delicate beginning is accomplished in the first place, nourishing the acceptance engine specifically from sun based PV cluster without beginning the MPPT exchanging of lift converter. When the machine accomplishes the speed of 1200 rpm, the MPPT is initiated through a lift converter and inside part of a moment the unfaltering state is come to. The DC connect voltage accomplishes its unfaltering state estimation of 600V and the sun powered PV accomplishes Vmp and Imp at 0.1s. The P&O calculation begins following the most extreme power point. Fig.5 examines the consistent state exhibitions of vector controlled acceptance engine drive at 1000W/m2. The principal waveform demonstrates the stationery rotor transition part (Ψr and Ψr) and resultant stationery motion (ω r) and the assessed synchronous speed (ω e) and slip speed (ω sl) from which the rotor speed (ω m) is evaluated.

Reference speed (ω m) is calculated by adding speed derived from Ppv i.e. (ω 1) and the voltage controller output (ω 2). The electromagnetic torque (Te) achieves its steady-state value of 12.5 Nm for 1000W/m2 very quickly with a limit of 18 Nm (within allowable range) and pump torque (Tp) follows the usual fashion but ultimately settles down at steady-state as shown in the figures. Fig.6 deals with the steady-state performance of motor-pump and it has been observed that motor performs smoothly.

B. Dynamic Performance of Proposed System

During Step Decrease in Variable Irradiance Fig.7 and Fig.8 represent the satisfactory performances of the overall system during variable insulation level. As one knows that there is nominal change in the PV open circuit voltage (Voc) as well as the PV voltage at maximum power (Vpv) as the insulation is changed. However, there is appreciable change in the short circuit current (Isc) and current at MPP (Ipv). This behavior is verified by Fig.7 in which the insolation level is reduced from 1000W/m2 to 400W/m2 from 0.6s to 0.62s. The satisfactory motor performance is observed during this variation in the insulation as shown in Fig.8.

C. Dynamic Performance of Proposed System

During Step Increase in Variable Irradiance Similar to past case, Fig.9 and Fig.10 demonstrate the agreeable exhibitions of the general framework amid step increment in factor irradiance from 400W/m2 to 1000W/m2. Table I demonstrates the extensive variety of enduring state execution of the drive and it is demonstrated that the SPV voltage (Vpv) remains relatively same. Be that as it may, the PV control limit demonstrates a decay as there is critical decrement in the PV current (Ipv). DC connect voltage (Vdc) stays steady as it is controlled and managed by vector-control of VSI nourished enlistment engine drive. The THDi (Total Harmonic Distortion of engine current) increments as the insolation reductions and productivity remain relatively same up to 500W/m2 yet after that it diminishes essentially.
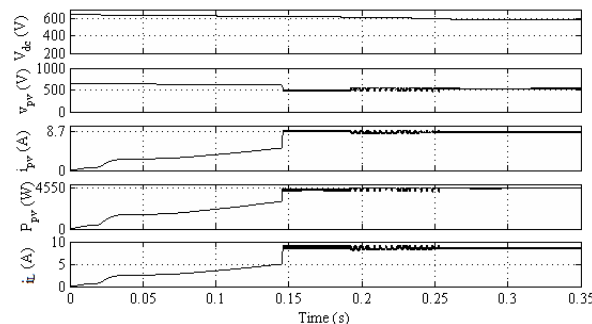

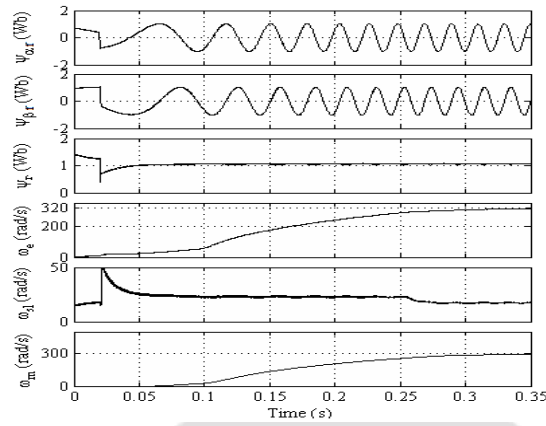Fig. 4. Starting and MPPT of solar PV fed system at 1000W/m2

Fig. 5. Motor speed estimation of induction motor drive through rotor fluxes in stationery reference frame at 1000W/m2 insulation
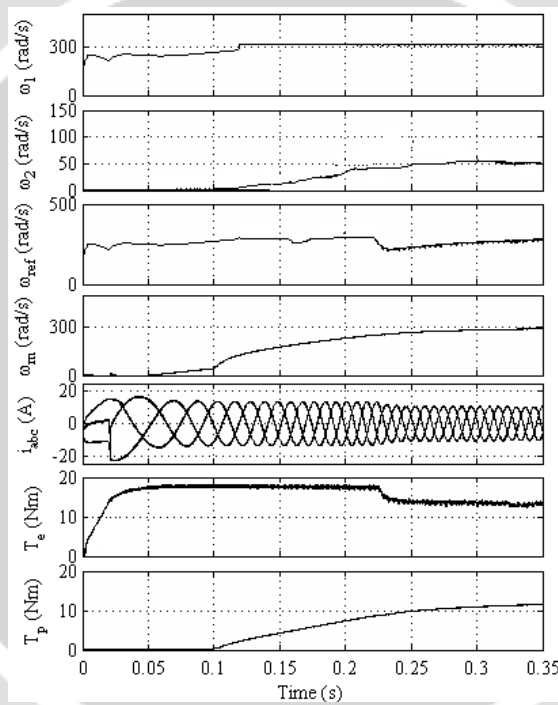

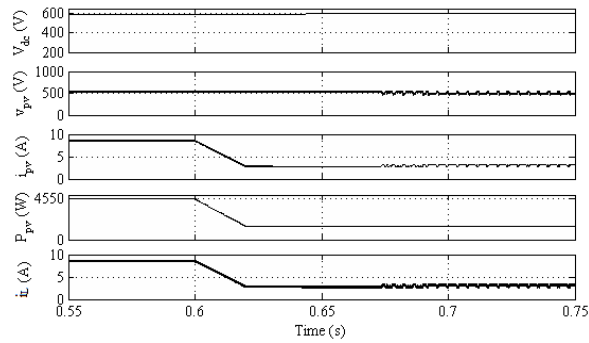Fig. 6. Starting and steady state operation of induction motor fed water pumping system at 1000W/m2

Fig. 7. Performance of the solar PV panel during decrease in insulation from 1000W/m2 to 400W/m2
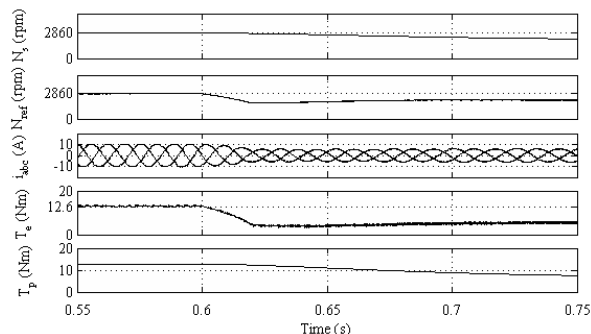
Fig. 8. Induction motor performance during decrease in insulation from 1000W/m2 to 400W/m2
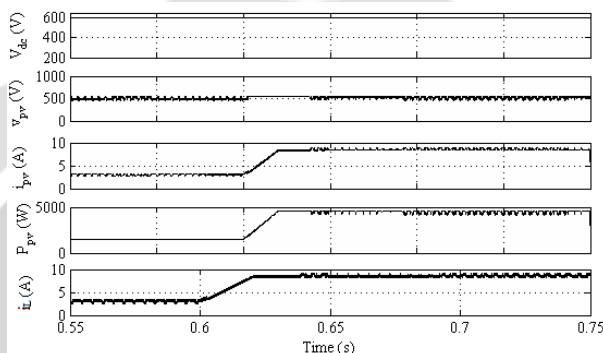

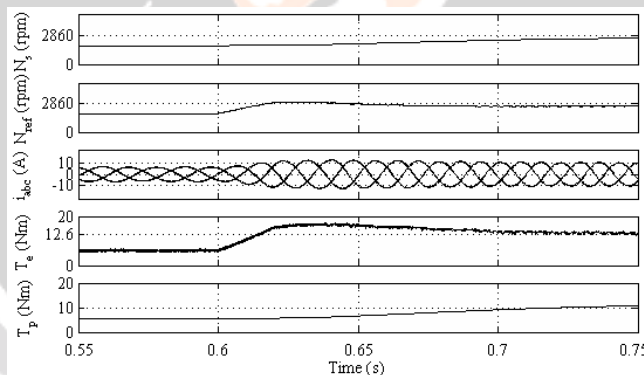Fig. 9. Performance of the solar PV panel during increase in insulation from 400W/m2 to 1000W/m2

Fig. 10. Induction motor performance of the system during increase in insulation from 400W/m2 to 1000W/m2

TABLE1
PERFORMANCE OF THE DRIVE AT DIFFERENT INSOLATION

Insolation (W/m^2)	P_{pv}(W)	V_{pv}(V)	I_{pv}(A)	Speed (rad/s)	Torque (Nm)	η in %	THD$_i$ (%)
1000	4510	541.4	8.7	299.3	12.7	83	2.56
800	3525	541.1	6.9	274	10.6	82.8	3.18
600	2510	540.8	5.15	243	8.7	82.6	3.88
400	1535	541	3.2	202	5.6	75.3	4.68

6. CONCLUSION

This paper manages a two phase sunlight based photovoltaic (SPV) bolstered speed sensor less vector controlled enlistment engine drive (IMD) for water pumping framework which is better than customary controlled

engine as it is less expensive and dependable. The advances in charge procedures have made the control exact on account of acceptance engine. This change prompted the use of acceptance engine in the vast majority of the applications. At the point when sun oriented power is utilized for providing the enlistment engine .The primary imperative is to supply it even with the transient amid turn on and varieties in stack. One regular practice is to gauge the motion from the terminal voltages and streams. The execution of the drive relies upon the exactness of the motion estimator. Normally the productivity of the acceptance engine drive (IMD) is high around the evaluated stack and decays at fractional stacking. However the productivity can be upgraded by working the engine at ideal transition by controlling the motion part of current. Alternate techniques like speed control by differing rotor protection are significantly less viable in contrast with vector control strategy since this strategy is pertinent to three-stage slip-ring acceptance engine only. The change in speed relies on both rotor circuit protection and load .Due to control misfortune in the protection ,this technique is utilized where speed changes are required for brief period as it were. speed control by post changing additionally not compelling due do this strategy is material to squirrel confine acceptance engine as it were. An altered annoy and watch (Pand O) calculation is utilized to track most extreme power from spv exhibit. Today, individuals are more worried about petroleum product fatigue and natural issues caused by regular power age and sustainable power sources than any time in recent memory. Among the inexhaustible assets, photovoltaic boards and wind generators are essential contenders. They have the benefit of being support and contamination free. The smooth beginning of the engine is achieved by vector control of an enlistment engine .The framework execution is recreated in matlab/simulink condition and the outcomes are contrasted and customary vector controlled IMD.

7. REFERENCES

[1] R. Foster, M. Ghassemi and M. Cota, Solar energy: Renewable energy and the environment, CRC Press, Taylor and francis Group, Inc. 2010.

[2] S. Parvathy and A. Vivek, "A photovoltaic water pumping system with high efficiency and high lifetime," Int. Conf. Advancements in Power and Energy (TAP Energy), pp.489-493, 24-26 June 2015.

[3] R. Kumar and B. Singh, " Buck-boost converter fed BLDC motor for solar PV array based water pumping," IEEE Int. Conf. Power Electron. Drives and Energy Sys. (PEDES)., 2014.

[4] Zhang Songbai, Zheng Xu, Youchun Li and Yixin Ni, "Optimization of MPPT step size in stand-alone solar pumping systems," IEEE Power Eng. Society Gen. Meeting, June 2006.

[5] H. Gonzalez, R. Rivas and T. Rodriguez, "Using an Artificial Neural Network as a Rotor Resistance Estimator in the Indirect Vector Control of an Induction Motor," IEEE Latin Amer. Trans, vol.6, pp.176-183, June 2008.

[6] Yen-Shin Lai, "Machine modeling and universal controller for vectorcontrolled induction motor drives," IEEE Trans. Energy Convers., vol.18, pp.23-32, Mar 2003.

[7] H. Abidi, A.B. Ben Abdelghani and D. Montesinos-Miracle, "MPPT algorithm and photovoltaic array emulator using DC/DC converters," IEEE Mediterranean Electrotechnical Conf. (MELECON), pp.567-572, 25-28 March 2012.

[8] A. Ali, Gu Yunjie, Xu Chi, Li Wuhua and He Xiangning, "Comparing the performance of different control techniques for DC-DC boost converter with variable solar PV generation in DC microgrid," IEEE confer. Ind. Electron. and Appli. (ICIEA), pp.603-609, 9-11 June 2014.

[9] N. Femia, G. Petrone, G. Spagnuolo and M. Vitelli, "Optimization of perturb and observe maximum power point tracking method," IEEE Transactions Power Electron., vol.20, pp.963-973, July 2005.

[10] D.G. Holmes, B.P. McGrath and S.G. Parker, "Current Regulation Strategies for Vector-Controlled Induction Motor Drives," IEEE Trans. Ind. Electron., vol.59, pp.3680-3689, Oct. 2012.

[11] FeiXu, Liming Shi and Yaohua Li, "The Weighted Vector Control of Speed-Irrelevant Dual Induction Motors Fed by the Single Inverter," IEEE Trans.Power Electron, vol.28, pp.5665-5672, Dec. 2013.

[12] Sonak Singh and Bhim Singh, "Solar PV water pumping system with DC link voltage regulation," Int. J. Power Electron., vol.7, no.1/2, 2015.

[13] M. Mengoni, L. Zarri, A. Tani, G. Serra and D. Casadei, "Stator Flux Vector Control of Induction Motor Drive in the Field Weakening Region," IEEE Trans. Power Electron., vol.23, pp.941-949, March 2008.

[14] B. Singh, Bhubaneswar and V.Garg, "A Novel Polygon Based 18- Pulse AC–DC Converter for Vector Controlled Induction Motor Drives," IEEE Trans.Power Electron., vol.22, pp.488-497, March 2007.

BIOGRAPHIES

	MOHD MUDASSIR HUSSAIN He received his bachelor's degree (B.E) from Osmania university, Telangana in July 2011.he is currently pursuing M.Tech (EPS) From Vidya Jyothi Institute Of Technology (Autonomous) (Jawaharlal Nehru Technology University) , Aziz Nagar Gate, C.B. Post ,Hyderabad ,.His Research Interest Include EPS, PQ And Facts.
	K.RAJEEV is an Assistant Professor working with Vidya Jyothi Institute of Technology, Hyderabad India in the Electrical and Electronics Engineering Department. His areas of interests are power systems & power electronics.
	P. NAGESWARA RAO is an Associate Professor working with Vidya Jyothi Institute of Technology, Hyderabad India in the Electrical and Electronics Engineering Department. His areas of interests are power systems & power electronics.